



Model biogas steam reforming in a thin Pd-supported membrane reactor to generate clean hydrogen for fuel cells



A. Iulianelli^a, S. Liguori^a, Y. Huang^b, A. Basile^{a,*}

^a Institute on Membrane Technology of Italian National Research Council (ITM-CNR), c/o University of Calabria Cubo 17/C, Rende, CS 87036, Italy

^b State Key Laboratory of Materials-oriented Chemical Engineering, College of Chemistry & Chemical Engineering, Nanjing University of Technology, Xin-Mo-Fan Road 5, Nanjing 210009, China

HIGHLIGHTS

- A Pd/Al₂O₃ membrane reactor generates concentrated H₂ (96%) via biogas reforming.
- The H₂/N₂ ideal perm-selectivity of the Pd/Al₂O₃ membrane is higher than 4000.
- The composite membrane reactor recovered 70% of H₂ during biogas reforming.

ARTICLE INFO

Article history:

Received 24 June 2014

Received in revised form

25 August 2014

Accepted 8 September 2014

Available online 16 September 2014

Keywords:

Biogas steam reforming

Membrane reactor

Clean hydrogen

Renewable sources

PEM fuel cells

ABSTRACT

Steam reforming of a model biogas mixture is studied for generating clean hydrogen by using an inorganic membrane reactor, in which a composite Pd/Al₂O₃ membrane separates part of the produced hydrogen through its selective permeation. The characteristics of H₂ perm-selectivity of the fresh membrane is expressed in terms of H₂/N₂ ideal selectivity, in this case equal to 4300. Concerning biogas steam reforming reaction, at 380 °C, 2.0 bar H₂O:CH₄ = 3:1, GHSV = 9000 h^{−1} the permeate purity of the recovered hydrogen is around 96%, although the conversion (15%) and hydrogen recovery (>20%) are relatively low; on the contrary, at 450 °C, 3.5 bar H₂O:CH₄ = 4:1, GHSV = 11000 h^{−1} the conversion is increased up to more than 30% and the recovery of hydrogen to about 70%. This novel work constitutes a reference study for new developments on biogas steam reforming reaction in membrane reactors.

© 2014 Elsevier B.V. All rights reserved.

1. Introduction

In the last decades, owing to a huge exploitation of fossil fuels to produce power, the rise of environmental pollution due to greenhouse gases (GHGs) and other harmful emissions has driven to the development of new technologies and to the utilization of renewable sources. Thus, hydrogen has been considered as a new and alternative energy carrier for several applications, making possible the development of the so called hydrogen economy [1,2]. Today, hydrogen generation comes from various feedstocks such as hydrocarbons, water and derived of biomass, involving several chemical processes and, consequently, energy requirements. Based on the nature of the chemical process and/or energy needs, hydrogen production can be realized mainly via thermochemical, electrochemical and/or biological methods [3]. However, nowadays

the dominant process for producing hydrogen at large scale is represented by the reforming of natural gas [4,5]; therefore, to solve the issues related to the formation of GHGs and to limit the exploitation of fossil fuels, it is expected that alcohols such as ethanol, methanol, glycerol or other bio-fuels as acetic acid, biogas etc. could have a major impact in the future applications.

1.1. Biogas as a renewable source for hydrogen generation

Biogas represents a versatile raw material for reforming processes, which can be used as an alternative to natural gas as fossil fuels source. Then, hydrogen generation from biogas could help to largely lower the GHGs emission. Commonly, the composition of biogas is based mainly on methane and carbon dioxide, besides traces of H₂S, NH₃, hydrogen, nitrogen, oxygen and steam [6]. The composition of each compound is not fixed and can vary depending on which kind of residual biomass among animal waste, sewage treatment plants or industrial wastewater, landfills, etc. is used during the anaerobic digestion process [7]. As reported in the open

* Corresponding author. Tel.: +39 0984 492013; fax: +39 0984 402103.

E-mail address: a.basile@itm.cnr.it (A. Basile).

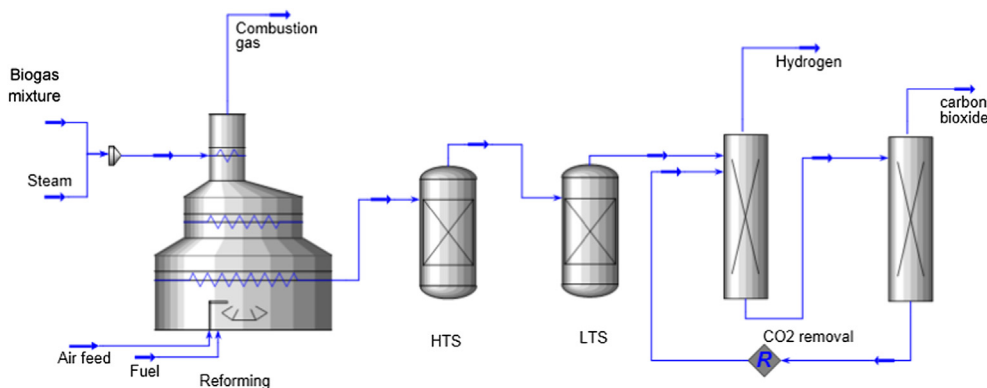


Fig. 1. Conceptual scheme of a conventional system for high grade hydrogen generation (HTS = high temperature water gas shift reactor; LTS = low temperature water gas shift reactor).

literature [8,9], in a biogas mixture methane can pass from 55% to 70%, carbon dioxide from 30% to 45%, H_2S from 500 to 4000 ppm, NH_3 from 100 to 800 ppm, while hydrogen, nitrogen, oxygen and steam can show percentage lower than 1% (vol.) with each one.

The biogas can be used in a wide range of applications [10], particularly because its chemical energy can be transformed into mechanical energy through combustion process. Furthermore, biogas can be useful to co-generate thermal energy, by producing hot water and steam through engines exercised at high temperature, or it can be burned to generate heat energy in boilers. Last but not least, it can be utilized directly as a fuel for automotive applications. However, even if at moment several types of biogas applications can be noticed, new and alternative routes of biogas exploitation could be followed. As a special case, biogas could be used to generate hydrogen to be further supplied to fuel cells [11,12], which reached remarkable progress in the last decade in the sector of transportation, for power generation and in stationary or portable installations [13–15].

1.2. Biogas reforming processes

Conventionally, in order to generate hydrogen the most common reforming processes involving methane (as a main product of biogas) are based on steam reforming, partial oxidation reforming, autothermal reforming, dry reforming and dry oxidation reforming [16]. Furthermore, in the open literature such non-conventional processes as solar reforming or thermal plasma reforming are noticed as further ways to produce hydrogen from methane [17,18]. Nevertheless, most of the scientific studies on biogas reforming for hydrogen generation deals with the utilization of model biogas mixtures in which only methane and carbon dioxide are present, whereas high purity methane (higher than 99%) is generally used to perform reforming reactions at bench scale. Indeed, to the best of our knowledge only few studies in the open literature regard the reforming of biogas directly coming from digestion process of residual biomass [19,20]. Therefore, as stated by Alves et al. [6], in a general subdivision when approaching to reforming of biogas, three different compositions of biogas should be taken into account: 1) *in natura*, with 55–70% of methane inside the mixture, 30–45% of CO_2 and 500–4000 ppm of H_2S ; 2) biogas partially treated to remove H_2S ; 3) purified biogas for “biomethane” enrichment (93–96% of methane, 4–7% of CO_2 and less than 20 ppm of H_2S).

However, hydrogen can be produced conventionally by methane or biogas reforming in a wide range of temperature between 600 and 1000 °C, which can be carried out at low pressure in fixed-bed (FBR) or fluidized bed reactors [21–24]. In this field, the combination of biogas reforming processes and fuel cells

represents an interesting route for generating clean energy, with added high-energy efficiency [6,25–27].

Commonly, most of the scientific articles from literature about steam reforming of biogas deals with the utilization of Ni-based catalyst [28–32] owing to its lower cost than Pt, Rh or Pd as noble metals-based catalysts [33–35]. Nevertheless, Ni shows a strong deactivation susceptibility to coke formation owing to the high temperatures normally used during steam reforming reaction, while Pt and Pd catalysts seem to be more adapt concerning the catalytic stability [6] as well as Rh showing greater catalytic activity than Ni associated to a lower coke formation tendency [36].

To produce high-grade hydrogen from biogas steam reforming, such formed products as CO and CO_2 besides other by-products should be separated. Typically, the purification of hydrogen in conventional processes is performed in, at least, three stages (Fig. 1): conventional reformer, water gas shift reactors (high and low temperature) and different separating units [37].

As a special field of interest, various scientific studies in literature deal with the benefits obtained by using hydrogen-selective membrane reactors (MRs), owing to the possibility of integrating the reaction and the hydrogen purification stage in a single processor, Fig. 2, with the further possibility of directly supplying fuel cells [37–44].

In this contest, Pd-based MR technology has been applied often to steam reforming of methane to produce high grade hydrogen [40,41,45–47], but – to the best of our knowledge – only one time directly to a biogas mixture [48]. Therefore, the aim of this manuscript is to investigate the production of high grade hydrogen from the steam reforming of a model biogas mixture by means of a supported Pd-based MR packed by a commercial Ni-based catalyst chosen for its low cost. The novelty of this work consists of the combination within the application of a composite membrane based on a thin Pd-layer deposited on a porous ceramic support and the exploitation of a renewable source as biogas mixture to generate clean hydrogen for fuel cells and, meanwhile, to decrease the emission of pollutants. In particular, the utilization of a composite Pd-based membrane, having quite high hydrogen perm-selectivity with respect to all other gases and lower cost than dense unsupported Pd-based membranes (owing to the lower content of palladium) could make possible to match the aforementioned objectives.

2. Experimental

The experimental setup consists mainly of the MR module in which a porous Al_2O_3 supported Pd-based membrane is allocated, Fig. 3. The producer of the composite Pd-based membrane is the Nanjing University of Technology, while the porous Al_2O_3 support

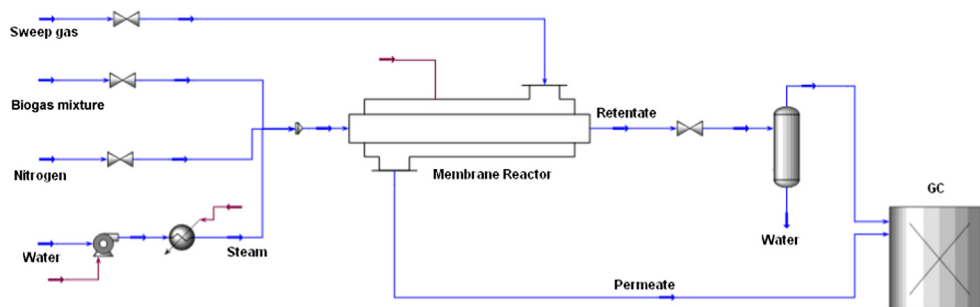


Fig. 2. Conceptual scheme of a membrane reactor for producing high grade hydrogen.

has been provided by Gao Q Funct. Mat. Co. The membrane, Fig. 4, is 75 mm of length and presents an external diameter around 13 mm and an internal diameter around 9 mm with an effective membrane area of ca. 17 cm². An homogeneous thin dense Pd-layer of around ~7 μm has been deposited via electroless plating on the substrate material constituted by a conventional porous α-Al₂O₃ with a symmetric structure, modified with γ-Al₂O₃ coating. However, the palladium morphology of the membrane is analyzed by a FEI Quanta-200 scanning electron microscopy (SEM). More details about the membrane preparation are reported elsewhere [49,50]. Furthermore, 0.5 g of Ni(25 wt%)/Al₂O₃ commercial catalyst have been packed in the annulus of the MR; before the reaction tests, the catalytic bed has been reduced by flowing for 2 h hydrogen and nitrogen (1.1×10^{-2} mol min⁻¹) at 300 °C. Concerning the reaction temperature used in this work, the MR has been exercised between 380 and 450 °C, while the reaction pressure has been varied from 2.0 bar to 3.5 bar, with the permeate pressure kept constant at 1.0 bar. The H₂O:CH₄ feed molar ratio ranged from 3:1 to 4:1, while the model biogas mixture used in this work has been constituted by CH₄ and CO₂ with ratio 60/40. The gas hourly space velocity (GHSV) has been varied during the tests from 9000 to 11000 h⁻¹.

The experimental plant at bench scale is constituted by a P680 HPLC pump (Dionex), useful for feeding deionized water, which is vaporized in a preheater and mixed with a constant flow rate of nitrogen (~21 mL min⁻¹), used as an internal standard gas, and with the model biogas mixture. Nitrogen is also flowed in the permeate side as a sweep-gas. CH₄, CO₂, N₂ and pure H₂ (the latter used for the catalyst reduction) are supplied by means of Brooks Instruments 5850S mass-flow controllers, driven by a Lira (Italy) software. Concerning the outlet streams, the retentate was cooled through a cold-trap (ice bath) to condensate the unreacted steam (in the whole experimental campaign regarding the reaction tests of this work, no permeation of steam was detected at the GC as a

product present in the permeate stream). Then, the gaseous streams coming from both permeate and retentate sides have been analyzed by a temperature programmed HP 6890 gas-chromatograph (GC), equipped with two thermal conductivity detectors at 250 °C and flowed by Ar as a carrier gas. The GC has been equipped by three packed columns: Porapak R 50/80 (8 ft × 1/8 inch) and CarboxenTM 1000 (15 ft × 1/8 inch) connected in series, and a Molecular Sieve 5 Å (6 ft × 1/8 inch). Each experimental point obtained in this work represents an average value of 10 experimental points taken in 140 min at steady-state condition with an error variation lower than 2%. The internal temperature of the MR has been checked with a thermocouple.

The MR performance during biogas steam reforming reaction have been evaluated by means of the following definitions:

$$\text{Methane conversion (\%)} = \frac{\text{CH}_{4-\text{in}} - \text{CH}_{4-\text{out}}}{\text{CH}_{4-\text{in}}} \times 100 \quad (1)$$

where CH_{4-in} and CH_{4-out} are the inlet and outlet methane flow rates, respectively.

$$\text{Hydrogen recovery (\%)} = \frac{\text{H}_{2-\text{permeate}}}{(\text{H}_{2-\text{permeate}} + \text{H}_{2-\text{retentate}})} \times 100 \quad (2)$$

where H_{2-permeate} and H_{2-retentate} are the hydrogen molar flow rates in the permeate and retentate sides, respectively.

$$\text{Hydrogen permeate purity (\%)} = \frac{\text{H}_{2-\text{permeate}}}{Q_{\text{permeate}}} \times 100 \quad (3)$$

where Q_{permeate} represents the total permeate molar flow rate.

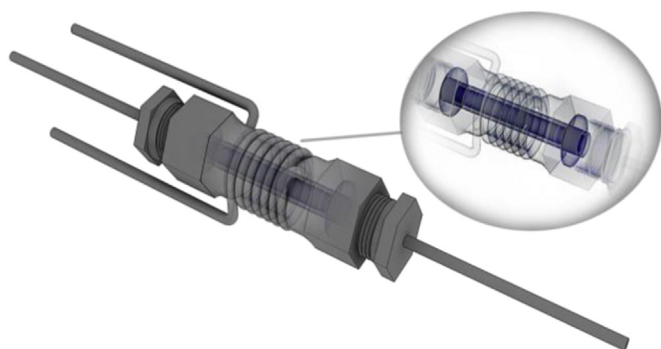


Fig. 3. Conceptual scheme of the membrane reactor allocating a composite Pd/Al₂O₃ membrane.



Fig. 4. The Pd/Al₂O₃ composite membrane.

Furthermore, the characterization to pure gas permeation of the composite Pd/Al₂O₃ membrane has been realized taking into account the equations reported below:

$$J_{H_2} = Pe \left(p_{H_2-\text{retentate}}^n - p_{H_2-\text{permeate}}^n \right) \quad (4)$$

Eq. (4) represents the general law regulating the hydrogen flux permeating through a generic membrane, where J_{H_2} indicates the hydrogen flux permeating through the composite membrane, Pe is the hydrogen permeance, $p_{H_2-\text{retentate}}$ and $p_{H_2-\text{permeate}}$ the hydrogen partial pressures in the retentate and permeate sides, respectively, n (variable in the range 0.5–1) the dependence factor of the hydrogen flux on the hydrogen partial pressure;

$$\alpha_{H_2/i} = \frac{J_{H_2}}{J_i} \quad (5)$$

where α_i represents the “ideal selectivity”, calculated as the ratio within the hydrogen permeating flux (J_{H_2}) over the permeating flux of another pure gas (J_i , with $i = N_2$ or He).

3. Results and discussion

3.1. Pure gas permeation tests

Prior to permeation tests, the membrane surface has been analyzed via SEM and Fig. 5 shows the characteristic cauliflower morphology of palladium. Furthermore, Fig. 6 reports the cross section of the membrane in order to point out the real thin palladium layer deposited onto the porous support.

Successively, pure gas permeation tests have been carried out on the composite Pd/Al₂O₃ membrane in order to establish its characteristics of H₂ perm-selectivity. In details, the permeation tests have been performed by flowing pure H₂, N₂ or He, respectively, at 380 °C and transmembrane pressure ranging between 0.5 and 1.0 bar. The results of the permeation tests at $\Delta p = 0.5$ bar are resumed in Table 1 as H₂/N₂ and H₂/He ideal selectivities and compared to the expected values from DOE target (2010). As shown, this table reports the ideal selectivities before and after the whole experimental campaign of reaction tests. Thus, in conditions of fresh membrane, the H₂/N₂ ideal selectivity was higher than 4000, lower but not so far from the correspondent DOE target (2010), which presents a value of 10000; furthermore, the H₂/He ideal selectivity was around 1500. Although the H₂ perm-selectivity values of the Pd/Al₂O₃ membrane seem to be interesting, in the meanwhile they also confirm that the composite membrane is not fully selective to hydrogen permeation and “ n ” of Eq. (4) cannot be assumed equal to 0.5 as a typical value of Sieverts–Fick law useful to describe the behavior of a H₂ full perm-selective membrane. As a consequence, to establish the right “ n ” for describing the hydrogen permeating flux through the membrane, the linear regression factor (R^2) at different “ n ” was evaluated. As shown in Fig. 7, the highest value of R^2 (0.9959) was reached at $n = 0.6$. This value is, then, inserted in the Eq. (4) to describe the hydrogen permeating flux through the Pd/Al₂O₃ membrane of this work as reported below.

$$J_{H_2} = Pe \left(p_{H_2-\text{retentate}}^{0.6} - p_{H_2-\text{permeate}}^{0.6} \right) \quad (6)$$

3.2. Reaction tests

Biogas steam reforming in the composite Pd/Al₂O₃ MR was initially carried out at 380 °C, 2.0 bar of reaction pressure, H₂O:CH₄ feed molar ratio equal to 3:1 and a GHSV = 9000 h^{−1}. As shown in Fig. 8, owing to the relatively low operating temperature, methane

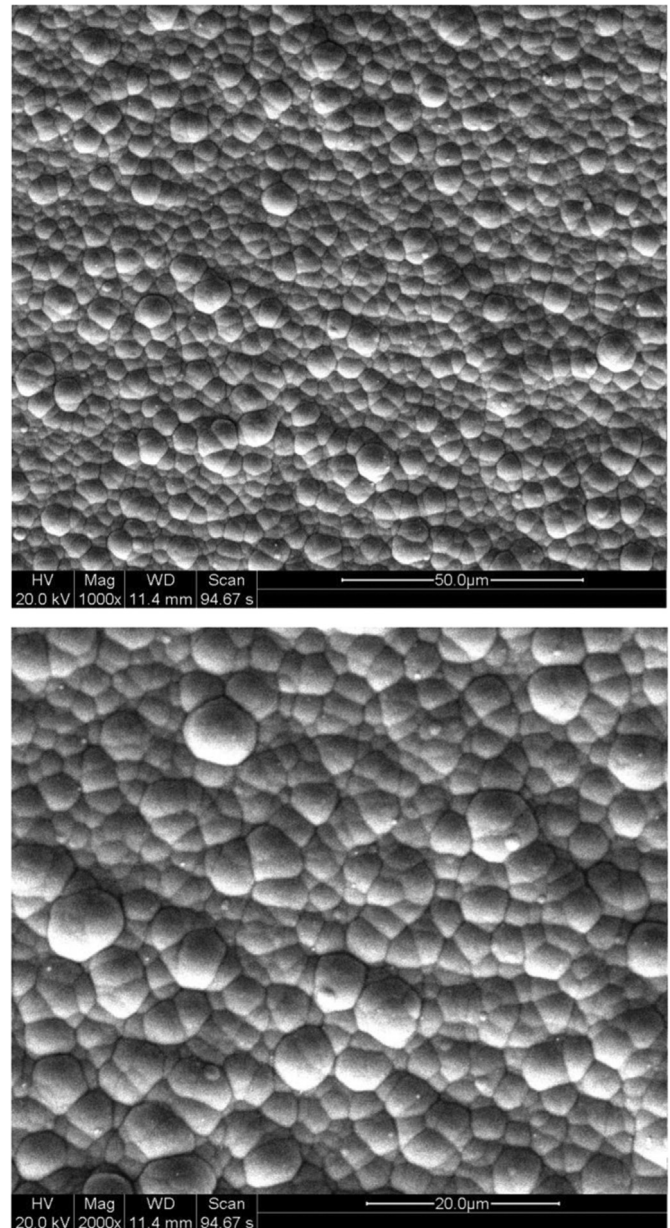


Fig. 5. SEM images of the composite membrane outer surface.

conversion was 27% and the hydrogen recovered in the permeate side lower than 30%, with a quite high purity of around 96%. Successively, to improve methane conversion, the reaction temperature was increased to 450 °C and the reaction pressure influence (in the range from 2.5 to 3.5 bar) on the MR performance was evaluated. Due to a higher temperature positively influencing the hydrogen permeability through the Pd-membrane [38], more hydrogen was removed from the reaction side and collected in the permeate side, consequently favoring an increase of both H₂ recovery and methane conversion, the latter due to the well-known shift effect [4]. Indeed, an increased temperature acts positively on biogas steam reforming because it is an endothermic reaction as well as enhances the hydrogen permeation through the membrane, emphasizing the aforementioned shift effect. Furthermore, an increase of reaction pressure makes possible greater hydrogen permeation driving force that, combined to the temperature effect, globally allows an enhancement of the H₂ recovery. In particular,

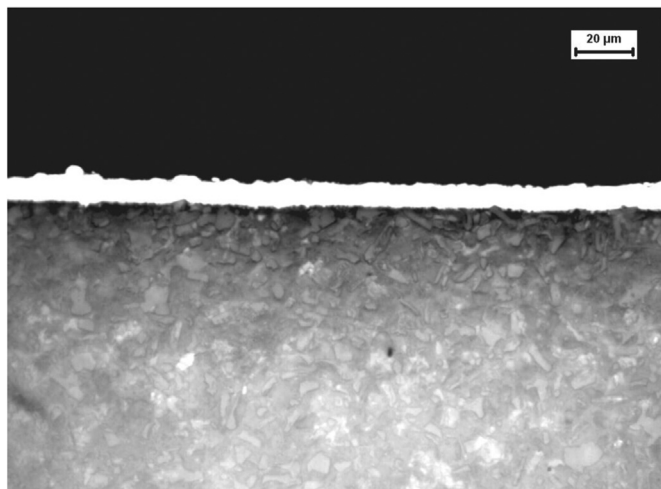


Fig. 6. SEM images of the cross section of the composite membrane.

Fig. 9 shows that, at 3.5 bar, methane conversion reached more than 30% with a hydrogen stream recovered in the permeate side equal to around 60%.

Now, as reported by Kolbitsch et al. [24], when a model biogas mixture is used for steam reforming reaction in FBRs packed with Ni-based catalysts, methane conversion increases by increasing temperature up to 750–800 °C. The same authors stated that, below 700 °C, normally it is relatively low. Unfortunately, the reaction temperature for the Pd/Al₂O₃ MR cannot be increased above 450 °C owing to the maximum temperature limit of the composite membrane. Therefore, on one hand a lower temperature favors an energy saving and limits dry reforming reaction [24], on the other hand methane conversion is depleted and the shift effect due to the selective permeation of hydrogen through the membrane does not compensate this loss of conversion. Then, further experimental tests were carried out to increase the feed molar ratio up to 4:1 at a space velocity of 11000 h⁻¹ and, at these conditions, Fig. 10 illustrates CH₄ conversion and H₂ recovery at 2.5 and 3.5 bar. From the theoretical point of view, the higher the space velocity the lower the conversion owing to a reduced residence time of the reactants in the catalytic bed. Nevertheless, Fig. 10 shows that, at 3.5 bar, methane conversion is higher than 30%, then superior to the conversion reached with GHSV = 9000 h⁻¹ because of using a higher feed molar ratio.

Concerning the H₂ permeate purity of the hydrogen recovered during the experimental tests (particularly referring to the results reported in Figs. 9 and 10), by referring to our previous study [55], it is possible to state that, owing to the effect of thermal cycles, the palladium was affected by an increase of pinholes formation, causing a depletion of the hydrogen perm-selectivity during the time. Indeed, Fig. 11 shows the trend of hydrogen permeate purity as a function of reaction pressure: its decrease is caused by a

combination of two effects, the presence of higher number of micro-defects on the palladium-surface as previously described and the higher flux of other products through the aforementioned defects, particularly emphasized at higher pressure. In fact, the composite Pd/Al₂O₃ membrane was globally exercised for around 1000 h and, as reported in Table 1, its hydrogen perm-selectivity characteristics in terms of H₂/N₂ and H₂/He ideal selectivities dramatically dropped at the end of the whole experimental campaign.

3.3. Optimization of biogas steam reforming in the Pd/Al₂O₃ membrane reactor

Having in mind industrial applications, the H₂ perm-selectivity stability and the membrane life are critical concerns regarding to the membrane commercialization. In fact, two relevant issues should be considered: the membrane quality and the membrane operation. The first one mainly depends on the characteristics of the membrane fabrication in terms of dimension of the layer and its uniformity, adhesion, local stress, presence of defects, etc. The second one relies to the membrane defects normally generated during long-term membrane operations. In particular, a higher operating temperature gradually leads to the sintering of the thin Pd-layers of composite membranes with a consequent higher percentage of defects creation. Therefore, all the aforementioned aspects could be the reason why the composite Pd/Al₂O₃ membrane of this work lost its initial H₂ perm-selectivity characteristics.

To optimize the potential applicability of the MR of this work to biogas steam reforming, two main choices about the operating conditions are possible. The first one regards the MR operation at low pressure (2.0 bar), temperature (380 °C) and GHSV (9000 h⁻¹). At these conditions, methane conversion (27%) and hydrogen recovery (27%) are relatively low, but the H₂ permeate purity (96%) is quite high (Fig. 12) and CO is completely absent, making useful this stream for PEM fuel cells applications. In this case, the produced H₂ present in the permeate stream is equal to 0.79 mL min⁻¹, while it is 2.14 mL min⁻¹ in the retentate. Furthermore, the loss of CH₄ for permeation through the membrane (0.03 mL min⁻¹ in the permeate stream over 13.8 mL min⁻¹ in the feed) does not affect the reaction performance significantly. The distribution of the retentate stream compositions (Fig. 13) shows that it is concentrated in CO₂ and could be further treated for CO₂ capture via polymeric membranes and/or other conventional systems (PSA).

The second option is at higher temperature (450 °C), reaction pressure (3.5 bar), GHSV (11000 h⁻¹) and feed molar ratio (H₂O:CH₄ = 4:1). Thus, the membrane is particularly stressed because the higher the working temperature the higher the possibility of sintering effect and consequent pinholes formation. Nevertheless, the conversion is higher than 30% and the hydrogen recovered is higher than 60%, although the loss of CH₄ for permeation in this case (0.84 mL min⁻¹ in the permeate stream over 13.8 mL min⁻¹ in the feed) depletes more consistently the reaction performance. Unfortunately, the higher the pressure the lower the H₂ permeate purity, which reached around 70% without CO content (Fig. 14), although the produced hydrogen present in the permeate stream at these operating conditions is improved up to 3.83 mL min⁻¹ over ~2.11 mL min⁻¹ in the retentate stream. By following the second option, the retentate stream is more concentrated in CO₂ than in the first case previously reported, Fig. 15.

In conclusion, in Table 2, by comparing the performance of various FBRs and MRs, it is possible to affirm that the MR of this work allowed to reach interesting results at milder conditions than referenced studies about FBRs. In this table, a qualitative comparison is proposed between FBRs and MRs. In particular, for the FBRs

Table 1
Hydrogen/other gas ideal selectivities for the composite Pd/Al₂O₃ membrane before and after reaction tests in comparison with the expected values from DOE target (2010); T = 380 °C and Δp = 0.5 bar.

Pure gas (i)	$\alpha_{H_2/i}$		
	Before reaction tests	After reaction tests	DOE target (2010)
H ₂	1	1	1
N ₂	$\sim 4.3 \times 10^3$	$\sim 1.0 \times 10^3$	1.0×10^4
He	$\sim 1.5 \times 10^3$	$\sim 4.3 \times 10^2$	—

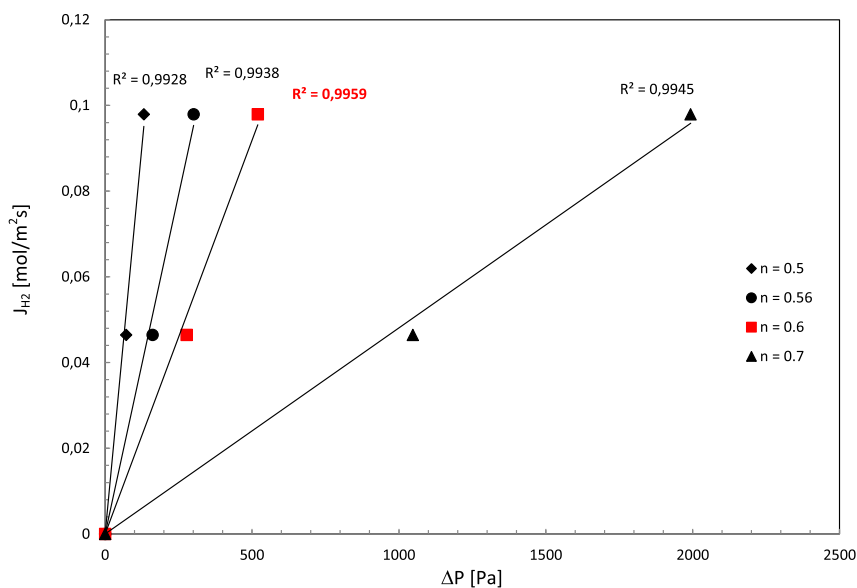


Fig. 7. Hydrogen permeating flux vs transmembrane pressure at different "n" and $T = 380^\circ\text{C}$.

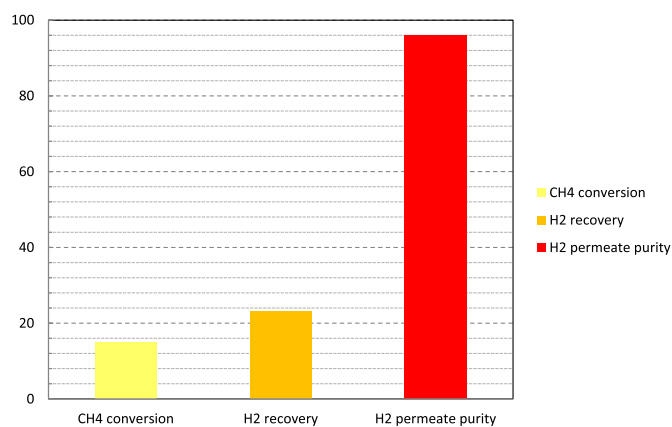


Fig. 8. Methane conversion, H₂ recovery and H₂ permeate purity for biogas steam reforming in a composite Pd/Al₂O₃ membrane reactor exercised at 380°C , $p = 2.0$ bar, $\text{H}_2\text{O}:\text{CH}_4 = 3:1$ and $\text{GHSV} = 9000\text{ h}^{-1}$.

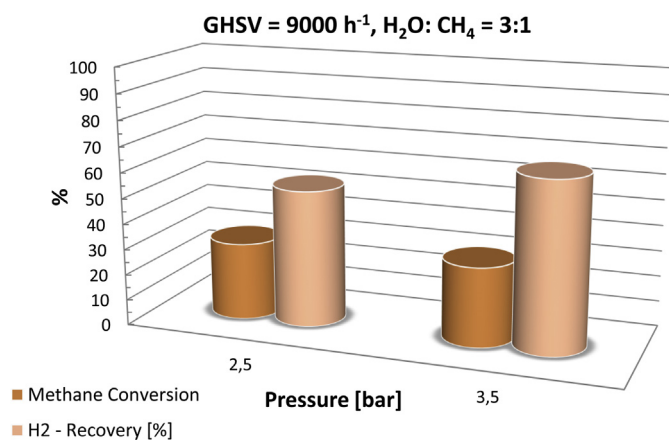


Fig. 9. Methane conversion and H₂ recovery at different reaction pressure for biogas steam reforming in a composite Pd/Al₂O₃ membrane reactor exercised at 450°C , $\text{H}_2\text{O}:\text{CH}_4 = 3:1$ and $\text{GHSV} = 9000\text{ h}^{-1}$.

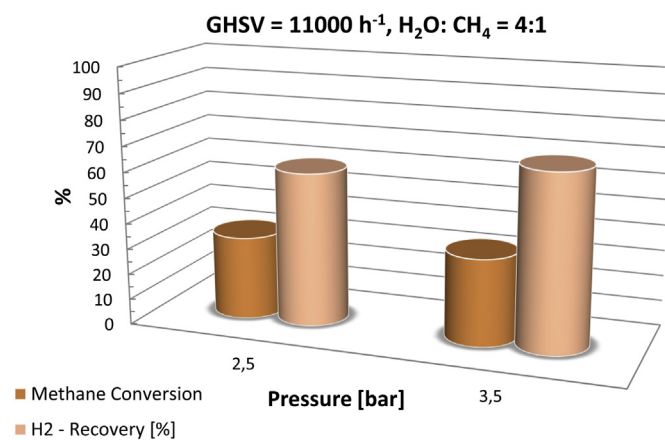


Fig. 10. Methane conversion and H₂ recovery at different reaction pressure for biogas steam reforming in a composite Pd/Al₂O₃ membrane reactor exercised at 450°C , $\text{H}_2\text{O}:\text{CH}_4 = 4:1$ and $\text{GHSV} = 11000\text{ h}^{-1}$.

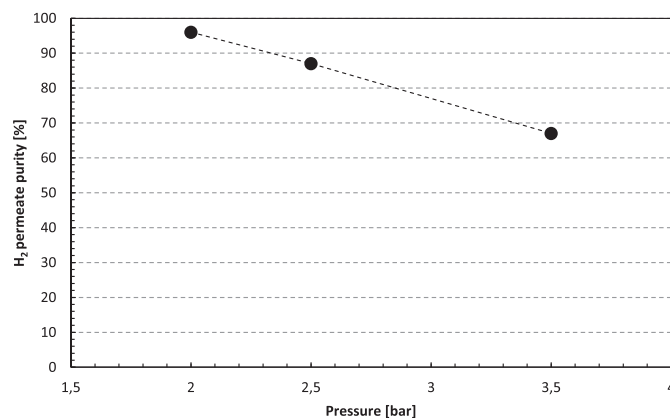


Fig. 11. H₂ permeate purity at various reaction pressure for biogas steam reforming in a composite Pd/Al₂O₃ membrane reactor exercised at 450°C , $\text{H}_2\text{O}:\text{CH}_4 = 4:1$ and $\text{GHSV} = 11000\text{ h}^{-1}$.

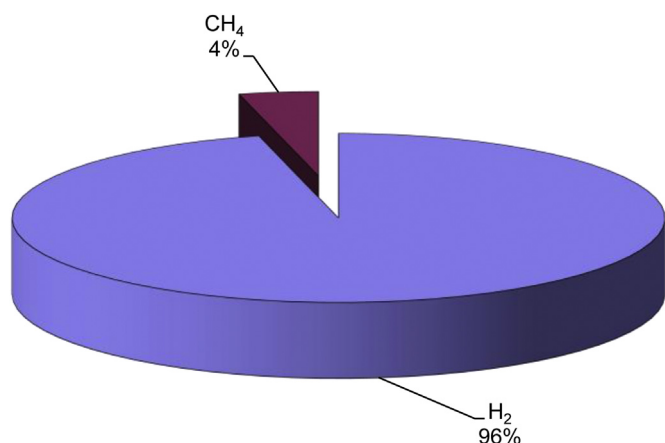


Fig. 12. Permeate product distribution during biogas steam reforming in a composite Pd/Al₂O₃ membrane reactor exercised at 380 °C, 2.0 bar of reaction pressure, 1.0 bar of permeate pressure, H₂O:CH₄ = 3:1 and GHSV = 9000 h⁻¹.

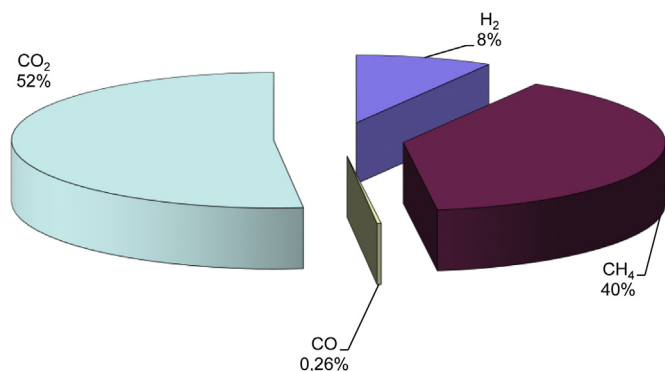


Fig. 13. Retentate product distribution during biogas steam reforming in a composite Pd/Al₂O₃ membrane reactor exercised at 380 °C, 2.0 bar of reaction pressure, 1.0 bar of permeate pressure, H₂O:CH₄ = 3:1 and GHSV = 9000 h⁻¹.

great methane conversions are achieved at temperature not lower than 600 °C. For example, Roh et al. [51] reached 70% of methane conversion at 600 °C by using a Ni-based catalyst, while Avraam et al. [54] reached 90% of conversion by using a Ru-based catalyst. At temperature lower than 600 °C, the conversion in FBRs drops dramatically, while the MRs show such conversion at so lower temperature, with important economic benefits derived by the energy saving, with the further advantage of producing clean hydrogen.

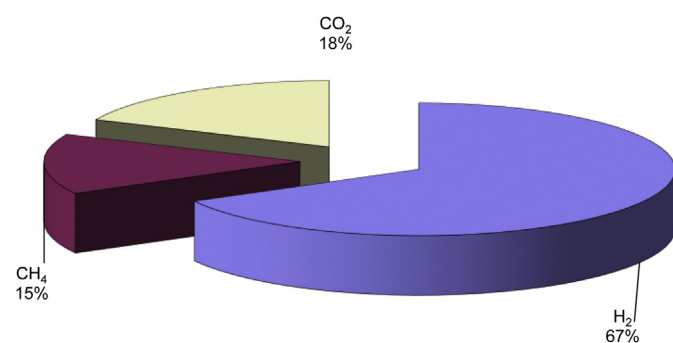


Fig. 14. Permeate product distribution during biogas steam reforming in a composite Pd/Al₂O₃ membrane reactor exercised at 450 °C, 3.5 bar of reaction pressure, 1.0 bar of permeate pressure, H₂O:CH₄ = 4:1 and GHSV = 11000 h⁻¹.

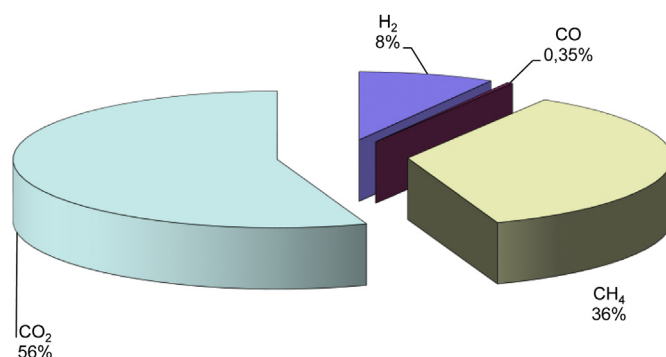


Fig. 15. Retentate product distribution during biogas steam reforming in a composite Pd/Al₂O₃ membrane reactor exercised at 450 °C, 3.5 bar of reaction pressure, 1.0 bar of permeate pressure, H₂O:CH₄ = 4:1 and GHSV = 11000 h⁻¹.

Conclusion and future trends

A model biogas mixture has been utilized in a steam reforming process performed in a composite Pd/Al₂O₃ MR to generate renewably clean hydrogen for possible fuel cells applications. This work represents a pioneering work on this thematic also considering that, to the best of our knowledge, only another study involving MRs is present in the open literature. Therefore, biogas steam reforming has been studied at low temperature achieving, at the best, conversion higher than 30% at 450 °C, 3.5 bar H₂O:CH₄ = 4:1, GHSV = 11000 h⁻¹ with a quite high hydrogen recovery around 70%. Unfortunately, at these conditions, owing to the increased presence of pinholes formation on the Pd-layer of the composite membrane during the MR operations, the characteristics of H₂ perm-selectivity were decreased, inducing a H₂ permeate purity lower than 70%. On the contrary, the MR operated at 380 °C, 2.0 bar, H₂O:CH₄ = 3:1, GHSV = 9000 h⁻¹ allowed a modest conversion (27%), but the hydrogen recovered in the permeate side (>20%) showed a purity around 96%. In all the investigated cases of this work, the retentate stream was concentrated in CO₂ useful for its capture. The main drawbacks individuated in this work is the loss of H₂ perm-selectivity of the membrane caused by the thermal cycles necessary to regenerate the catalyst and the operating temperature close to the maximum limit that caused formation of pinholes and Pd-layer sintering. Indeed, after 1000 h under operation, the MR of this work lost around 25% the initial characteristics of H₂/N₂ ideal selectivity (final value 1.0 · 10³). Therefore, as a future

Table 2

Qualitative comparison among performance of fixed bed reactors (FBRs) and membrane reactors (MRs) for biogas steam reforming reaction.

Kind of reactor	Temperature [°C]	Catalyst	CH ₄ conversion [%]	H ₂ recovery [%]	Ref.
FBR	600	Ni/Ce _{0.8} Zr _{0.2} O ₂	70	—	Roh et al. [51]
FBR	650	NiMg _{17.4} Al _{1.6} O _{20.8}	98	—	Fonseca et al. [52]
FBR	700	Ni/Al ₂ O ₃	85	—	Maluf and Assaf [53]
FBR	715	Ru/Al ₂ O ₃	90	—	Avraam et al. [54]
FBR	750	Ni/Al ₂ O ₃	85	—	Effendi et al. [21]
MR	450	Ru/Al ₂ O ₃	—	11%	Sato et al. [48]
MR ^a	380	Ni/Al ₂ O ₃	15	23	This work
MR ^b	450	Ni/Al ₂ O ₃	34%	~70%	This work

^a Reaction pressure = 2.0 bar, H₂O:CH₄ = 3:1, GHSV = 9000 h⁻¹.

^b Reaction pressure = 3.5 bar, H₂O:CH₄ = 4:1, GHSV = 11000 h⁻¹.

trend, the stability of the perm-selectivity characteristics of the membrane should be enhanced, also considering to enlarge the maximum temperature limit of the membrane. Furthermore, the use of a real biogas mixture will constitute the up-date of this work, by simulating real conditions during biogas steam reforming and by evaluating the effect of such contaminants on the MR performance.

Acknowledgments

The Authors would like to thank the Italian Ministry of Economic Development (MISE) for the funds received by Microgen30 project, contract number EE01_00013, to develop part of the research of this work.

Acronyms

DOE	Department of Energy
FBR	Fixed Bed Reactor
GC	Gas Chromatograph
GHG	Greenhouse Gases
GHSV	Gas Hourly Space Velocity
HTS	High Temperature Shift (reactor for water gas shift carried out at high temperature)
LTS	Low Temperature Shift (reactor for water gas shift carried out at low temperature)
MR	Membrane Reactor
PEM	Proton Exchange Membrane
PSA	Pressure Swing Adsorption
SEM	Scanning Electron Microscopy

Symbols

J	permeating Flux
n	dependence factor of the hydrogen flux on the hydrogen partial pressure
p	Partial pressure
P_e	Hydrogen permeance
Q	molar flow rate
Δp	transmembrane pressure
α	ideal selectivity

References

- [1] R. Chaubey, S. Sahu, O.O. James, S. Maity, *Renewable Sustainable Energy Rev.* 23 (2013) 443–462.
- [2] T.R. Nielsen, *Catal. Today* 106 (2005) 293–296.
- [3] J.A. Turner, *Science* 305 (2004) 972–974.
- [4] A. Iulianelli, S. Liguori, T. Longo, A. Basile, in: Damon Robert Honery, Patrick Moriarty (Eds.), *Hydrogen Production: Prospects and Processes*, Series: Energy Science, Engineering and Technology, Nova Science Publishers, Victoria, Australia, 2012, ISBN 978-1-62100-246-8, pp. 377–398 (Chapter 12).
- [5] P. Moriarty, D. Honnery, *Int. J. Hydrogen Energy* 32 (2007) 1616–1624.
- [6] H.J. Alves, C. Bley Jr., R.R. Niklevicz, E.P. Frigo, M.S. Frigo, C.H. Coimbra-Araújo, *Int. J. Hydrogen Energy* 38 (2013) 5215–5225.
- [7] N. Muradov, F. Smith, *Energy Fuels* 22 (2008) 2053–2060.
- [8] C.S. Lau, A. Tzolankis, M.L. Wyszynski, *Int. J. Hydrogen Energy* 36 (2011) 397–404.
- [9] A. Effendi, K. Hellgardt, Z.-G. Zhang, T. Yoshida, *Fuel* 84 (2005) 869–874.
- [10] M. Pöschl, S. Ward, P. Owende, *Appl. Energy* 87 (2010) 3305–3321.
- [11] D.D. Papadakis, S. Ahmed, R. Kumar, *Energy* 44 (2012) 257–277.
- [12] J.V. Herle, Y. Membrez, O. Bucheli, *J. Power Sources* 127 (2004) 300–312.
- [13] K.D. Kreuer, *J. Membr. Sci.* 185 (2001) 29–39.
- [14] A. Iulianelli, A. Basile, *Int. J. Hydrogen Energy* 37 (2012) 15241–15255.
- [15] O.Z. Sharaf, M.F. Orhan, *Renewable Sustainable Energy Rev.* 32 (2014) 810–853.
- [16] A. Basile, S. Liguori, A. Iulianelli, in: A. Basile, G. Mills, F. Hai, L. Di Paola (Eds.), *Membrane Reactors for Energy Applications and Basic Chemical Production*, Woodhead Publishing Ltd, 2014 submitted for publication.
- [17] C. Agrafiotis, H. von Storch, M. Roeb, C. Sattler, *Renewable Sustainable Energy Rev.* 29 (2014) 656–682.
- [18] Y.N. Chun, Y.C. Yang, K. Yoshikawa, *Catal. Today* 148 (2009) 283–289.
- [19] S. Araki, N. Hino, T. Mori, S. Hikazudani, *J. Nat. Gas. Chem.* 19 (2010) 477–481.
- [20] T. Okubo, Y. Hideschima, Y. Shudo, *Int. J. Hydrogen Energy* 35 (2010) 13021–13027.
- [21] A. Effendi, Z.-G. Zhang, K. Hellgardt, K. Honda, T. Yoshida, *Catal. Today* 77 (2002) 181–189.
- [22] L. Bollini Braga, J.L. Silveira, M.E. da Silva, C.E. Tuna, E.B. Machin, D.T. Pedrosa, *Renewable Sustainable Energy Rev.* 28 (2013) 166–173.
- [23] U. Izquierdo, V.L. Barrio, N. Lago, J. Requies, J.F. Cambra, M.B. Güemez, P.L. Arias, *Int. J. Hydrogen Energy* 37 (2012) 13829–13842.
- [24] P. Kolbitsch, C. Pfeifer, H. Hofbauer, *Fuel* 87 (2008) 701–706.
- [25] A. Galvagno, V. Chiodo, F. Urbani, F. Freni, *Int. J. Hydrogen Energy* 38 (2013) 3913–3920.
- [26] A.L. da Silva, L.F.P. Dick, I.L. Müller, *Int. J. Hydrogen Energy* 37 (2012) 6580–6600.
- [27] A.A. Iordanidis, P.N. Kechagiopoulos, S.S. Voutetakis, A.A. Lemonidou, I.A. Vasalos, *Int. J. Hydrogen Energy* 31 (2006) 1058–1065.
- [28] S. Appari, V.M. Janardhanan, R. Bauri, S. Jayanti, O. Deutschmann, *Appl. Catal. A* 471 (2014) 118–125.
- [29] B. Saha, A. Khan, H. Ibrahim, R. Idem, *Fuel* 120 (2014) 202–217.
- [30] K.-H. Lin, H.-F. Chang, A.C.-C. Chang, *Int. J. Hydrogen Energy* 37 (2012) 15696–15703.
- [31] S. Araki, N. Hino, T. Mori, S. Hikazudani, *Int. J. Hydrogen Energy* 34 (2009) 4727–4734.
- [32] J. Xu, W. Zhou, Z. Li, J. Wang, J. Ma, *Int. J. Hydrogen Energy* 35 (2010) 13013–13020.
- [33] S. Damyanova, B. Pawelec, K. Arishtirova, J.L.G. Fierro, *Int. J. Hydrogen Energy* 36 (2011) 10635–10647.
- [34] A.F. Lucrédio, J.M. Assaf, E.M. Assaf, *Fuel Process. Technol.* 102 (2012) 124–131.
- [35] U. Izquierdo, V.L. Barrio, K. Bizkarra, A.M. Gutierrez, J.R. Arraibi, L. Gartzia, J. Bañuelos, I. Lopez-Arbeloa, J.F. Cambra, *Chem. Eng. J.* 238 (2014) 178–188.
- [36] F. Barrai, T. Jackson, N. Whitmore, M.J. Castaldi, *Catal. Today* 129 (2007) 391–396.
- [37] A. Iulianelli, P. Ribeirinha, A. Mendes, A. Basile, *Renewable Sustainable Energy Rev.* 29 (2014) 355–368.
- [38] A. Basile, A. Iulianelli, T. Longo, S. Liguori, M. De Falco, in: L. Marrelli, M. De Falco, G. Iaquaniello (Eds.), *Membrane Reactors for Hydrogen Production Processes*, Springer, London Dordrecht Heidelberg New York, 2011, ISBN 978-0-85729-150-9, pp. 21–55, <http://dx.doi.org/10.1007/978-0-85729-151-6> (Chapter 2).
- [39] A. Basile, A. Iulianelli, S. Liguori, in: V. Piemonte, M. De Falco, A. Basile (Eds.), *Sustainable Development in Chemical Engineering*, Wiley, Chichester, West Sussex, 2013, ISBN 9781119953524, pp. 119–151.
- [40] A. Basile, S. Campanari, G. Manzolini, A. Iulianelli, T. Longo, S. Liguori, M. De Falco, V. Piemonte, *Int. J. Hydrogen Energy* 36 (2011) 1531–1539.
- [41] A. Iulianelli, G. Manzolini, M. De Falco, S. Campanari, T. Longo, S. Liguori, A. Basile, *Int. J. Hydrogen Energy* 35 (2010) 11514–11524.
- [42] G.Q. Lu, J.C. Diniz-Costa, M. Dukec, S. Giessler, R. Socolowe, R.H. Williams, et al., *J. Colloid Interf. Sci.* 314 (2007) 589–603.
- [43] Y. Lin, S. Liu, C. Chuanga, Y. Chub, *Catal. Today* 82 (2003) 127–139.
- [44] A. Brunetti, E. Drioli, P. Barbieri, *Fuel Process. Technol.* 118 (2014) 278–286.
- [45] L. Barelli, G. Bidini, F. Gallorini, S. Servili, *Energy* 33 (2008) 554–570.
- [46] J. Tong, Y. Matsumura, *Appl. Catal. A* 286 (2005) 226–231.
- [47] Y. Chen, Y. Wang, H. Xu, G. Xiong, *Appl. Catal. B Environ.* 80 (2008) 283–294.
- [48] T. Sato, T. Suzuki, M. Aketa, Y. Ishiyama, K. Mimura, N. Itoh, *Chem. Eng. Sci.* 65 (2010) 451–457.
- [49] X. Hu, W. Chen, Y. Huang, *Int. J. Hydrogen Energy* 35 (2010) 7803–7808.
- [50] Y. Huang, X. Hu, W. Chen, *US Patent* 8445055, 2009.
- [51] H.S. Roh, I.H. Eum, D.W. Jeong, *Renewable Energy* 42 (2012) 212–216.
- [52] A. Fonseca, E.M. Assaf, *J. Power Sources* 142 (2005) 154–159.
- [53] S.S. Maluf, E.M. Assaf, *Fuel* 88 (2009) 1547–1553.
- [54] D.G. Avraam, T.I. Halkides, D.K. Liguras, O.A. Berekrtidou, M.A. Goula, *Int. J. Hydrogen Energy* 35 (2010) 9818–9827.
- [55] S. Liguori, A. Iulianelli, F. Dalena, P. Pinacci, F. Drago, M. Broglia, Y. Huang, A. Basile, *Membranes* 4 (2014) 143–162.